

Simple Calibration Technique for Phased Array Radar Systems

Galina Babur^{1, 2, *}, Gleb O. Manokhin¹, Evgeniy A. Monastyrrev³,
Andrey A. Geltser¹, and Alexander A. Shibelgut^{1, 4}

Abstract—This paper presents a novel effective calibration technique applicable to phased array radars. The real embedded patterns of the array elements are measured independently in operating mode, taking antenna coupling and other parasitic effects into account. The proposed calibration technique requires minimal modification of the radar hardware. A set of angular-dependent error coefficients, which are compensated during the calibration process, are extracted for one received pulse for one/each angular direction of interest. The performance and effectiveness of the here-proposed calibration technique are assessed by means of modeling and experimental verification.

1 Introduction

2 Received Signal Model

3 Calibration Technique

3.1 Description

3.2 Important Notes

4 Validation of the Proposed Calibration Technique

5 Conclusion

Acknowledgment

References

1. INTRODUCTION

In phased array radars with electronic beam-steering, excitation phase and amplitude of the array elements are adjusted electronically in order to shape and point the array pattern along the desired direction [1, 2]. Phase and amplitude errors introduced in the beam-forming network can lead to a degradation of the array pattern characteristics in terms of increased sidelobe level and reduction of peak directivity [3, 4]. Coupling is present in all antenna arrays to some extent and can significantly affect their operation [5]. Besides, the non-ideality of the radiation pattern featured by the individual array elements results in a non-uniform radiation/reception of the radio signal along different angular directions [6].

Calibration is necessary because it reduces the array errors. The smaller the array errors are, the closer the implemented radiation pattern is to the theoretical pattern of the phased array.

Received 12 October 2016, Accepted 8 February 2017, Scheduled 23 March 2017

* Corresponding author: Galina Babur (galinababur@gmail.com).

¹ Department of Telecommunications and Radio-engineering Fundamentals, TUSUR, 40 Lenin Avenue, Tomsk, Russia. ² Simon Stevin Institute for Geometry, Nottebohmstraat 8, 2018 Antwerpen, Belgium. ³ Institute of Semiconductor Devices (NIIPP), Tomsk, Russia. ⁴ Department of Computer Measuring Systems and Metrology, TPU, 30 Lenin Avenue, Tomsk, Russia.

The errors in a phased array transceiver can be classified into two groups, static and dynamic [7]. Static errors are due to differences in component tolerances and build quality of the array structure. Dynamic errors are caused by the fact that the characteristics of electronic components vary with temperature and can drift over time [8]. So, active phased array antennas require periodic recalibration throughout the deployment period.

The phased array theory is based on the coherent summation of signals. If excitation phases and amplitudes drift in unison, the array performance is not impacted. Only relative changes on phase and amplitude across radiated/received signals affect the array pattern characteristics [9]. Therefore, the array calibration can be performed by simply correcting the relative differences between signal phases and amplitudes [10].

In this work, we present a simple but effective technique for the calibration of phase and amplitude errors introduced at antenna element level in phased array radars with beamforming on receive. We assume that the rest of the hardware operates in an ideal manner. We consider a radar system consisting of a linear array of identical antennas under the assumption of a narrowband sounding signal. The signal processing relies on pulse compression of the processed signals.

Due to the reciprocity principle, the here-proposed technique can be applied both in transmit and receive modes. In both cases, the calibration coefficients are obtained by suitable processing of the signals in the receive chain. In this work, we demonstrate the applicability of the proposed methodology in receive mode only. Measurements are carried out in operating mode of the phased array radar. No separate measurements of the embedded radiation patterns or coupling between the array elements are required, which leads to a significant simplification of the calibration procedure. Therefore, we call our technique ‘simple’. A small amount of measurements (basically, one received pulse for one/each angular direction), is needed for extraction of the calibration coefficients.

The paper is organized as follows. The angular receive diagram, which includes the beamformed patterns in all angular directions of interest, is considered in Section 2. The coupling between the array elements and their embedded patterns is taken into account. Section 3 introduces the calibration technique. The experimental validation is presented in Section 4. Section 5 contains the conclusions.

2. RECEIVED SIGNAL MODEL

The considered radar system consists of a linear array of N identical antennas. The array can be equidistant or non-equidistant. All the array elements have the same theoretical (ideal) embedded pattern $P_0(\theta)$. The ideal pattern $P_0(\theta)$ has the width $(\theta_{\min} \dots \theta_{\max})$ at -3 dB level. We consider the beamformed angular directions within this width.

The ideal sum signal received by a linear antenna array in the absence of noise and mutual coupling between the elements can be written as:

$$s_{R,0}(t, \theta) = \sum_{n=1}^N P_0(\theta) \cdot e^{-j\vec{k}(\theta) \cdot \vec{x}(n)} \cdot s(t), \quad (1)$$

where $s(t)$ is the complex envelope of a sounding signal (the sounding waveform), e.g., a linear frequency modulated (LFM) waveform, N the number of receiving elements, k the wave vector, $\vec{x}(n)$ the position vector of the n th receiving element $n \in [1 \dots N]$, and θ the angular position of a hypothetical target.

In reality, the array elements have non-ideal embedded patterns $P_n(\theta)$, and the coupling between the array elements affects the received signals. Non-idealities of the phase shifters can affect the complex amplitudes of the processed signals. However, mismatches introduced by the phase shifters are not the only reason for possible differences between the received signals. The received signals are multiplied with the embedded patterns, which can be affected by the edge diffraction, mismatch, and variations in elements themselves and, therefore, can differ for each array element. Antenna mutual coupling can also affect the radiation patterns and modify the original distribution [12]. Our calibration technique takes all those errors into account, because it is performed during the operation mode of the phased array under test. When all N channels are operating, the phased shifters are functioning, and the mutual coupling is affecting the signals.

The coupling between the array elements can be modeled as a linear system via the mutual coupling matrix, because of the linearity in Maxwell’s equations [11]. The $(N \times 1)$ phased array can be simulated

with the $N \times N$ coupling matrix on receive,

$$\mathbf{R} = \begin{bmatrix} 1 & \rho_{12} & \dots & \rho_{1N} \\ \rho_{21} & 1 & \ddots & \rho_{2N} \\ \vdots & \ddots & \ddots & \vdots \\ \rho_{N1} & \rho_{N2} & \dots & 1 \end{bmatrix}, \quad (2)$$

which is a complex symmetrical matrix, because for the coupling coefficients $\rho_{nm} = \rho_{mn}$, and $|\rho_{nm}| < 1$, when $n \neq m$. The coupling of each element with itself (when $n = m$, the main diagonal of the matrix) is considered equal to one.

The beamforming process (phased shifters operation) adds a term $e^{+j\vec{k}(\theta_0) \cdot \vec{x}(n)}$ to the received signal components, where θ_0 is the beamformed angular direction, $\theta_0 \in (\theta_{\min} \dots \theta_{\max})$. The proposed technique requires the use of a point target for the calibration process. This target can be active or traditional passive, artificial or natural. However, the signal received from the calibration target should be strong enough to neglect possible signals scattered from other objects. For one/each measurement, the angular position of the point target used for calibration is known and equal to the beamformed direction, $\theta = \theta_0$. Since the target direction and beamformed direction coincide during the calibration process, we use only the symbol θ_0 hereafter.

The real signal received by the n th antenna element after appropriate phase shifting due to the beamforming can be written as:

$$s_{R,\theta_0}^n(t) = \sum_{m=1}^N P_m(\theta_0) \cdot \mathbf{R}(n, m) \cdot e^{-j\vec{k}(\theta_0) \cdot \vec{x}(m)} \cdot e^{+j\vec{k}(\theta_0) \cdot \vec{x}(n)} \cdot s(t). \quad (3)$$

where index m denotes the order number of the receiving element, similar to n , but is used for introduction of the coupling effects. Due to the coupling, one/each signal received by the n th antenna element in Eq. (3) is influenced not by one, but by all N radiation patterns ($m = 1, \dots, N$). The exponents $e^{-j\vec{k}(\theta_0) \cdot \vec{x}(m)} \cdot e^{+j\vec{k}(\theta_0) \cdot \vec{x}(n)} = e^{-j\vec{k}(\theta_0) \cdot (\vec{x}(m) - \vec{x}(n))}$ represent the propagation path term between the n th antenna and all the array elements including the element itself (one of the values m is equal to n). The coupling coefficient and the propagation path term for the n th antenna element regarding itself ($m \equiv n$) are equal to one. Eq. (3) can be written as follows:

$$s_{R,\theta_0}^n(t) = \left(P_n(\theta_0) + \sum_{m \neq n} P_m(\theta_0) \cdot \mathbf{R}(n, m) \cdot e^{-j\vec{k}(\theta_0) \cdot (\vec{x}(m) - \vec{x}(n))} \right) \cdot s(t), \quad (4)$$

to demonstrate how the mutual coupling contribution (the sum term) can modify the original patterns $P_n(\theta_0)$. Without the coupling effects, the signal received by the n th antenna element in Eq. (4) turns into $P_n(\theta_0) \cdot s(t)$.

It is known that changes in the absolute values of the phase and amplitude do not affect the array beam pattern. Only changes in the relative phase and amplitudes between elements influence the array pattern characteristics [9]. For extraction of these relative changes, the sum signal received by all the array elements can be written as:

$$s_{R,\theta_0}(t) = \sum_{n=1}^N \left(\frac{A(n, \theta_0)}{P_0(\theta_0)} \right) \cdot P_0(\theta_0) \cdot s(t), \quad (5)$$

where the relative difference between the real and ideal embedded patterns is described by the ratio $E(n, \theta_0) = A(n, \theta_0)/P_0(\theta_0)$, which we call the relative error coefficients. The coefficients $A(n, \theta_0) = \sum_{m=1}^N P_m(\theta_0) \cdot \mathbf{R}(n, m) \cdot e^{-j\vec{k}(\theta_0) \cdot (\vec{x}(m) - \vec{x}(n))}$ denote the real embedded patterns affected by the coupling effects. In the ideal case, when the real and ideal patterns are the same, the relative error coefficients $E(n, \theta_0) = 1$ or 0 dB. Once the coefficients $A(n, \theta_0)$ are known (measured), the relative error coefficients $E(n, \theta_0)$ can be calculated.

3. CALIBRATION TECHNIQUE

3.1. Description

We propose the application of time offsetting to the element wise received signals according to the circulating signal principle [12]. This principle is known for the possibility of digital transmit beamforming with the use of only one sounding waveform. With the relative time offset δt introduced into the received signal components before their summation, the aggregate signal received from the point calibration target can be written as follows:

$$s_{R,\theta_0}(t) = \sum_{n=1}^N A(n, \theta_0) \cdot s(t - (n-1) \cdot \delta t), \quad (6)$$

where θ_0 is the angular direction of this target, which is known a priori. The ideal (theoretical) radiation pattern of one/each array element $P_0(\theta)$, contributing to the coefficients $A(n, \theta_0)$, is supposed to be known in each considered angular direction $\theta = \theta_0$.

The introduced time offset δt is inversely proportional to the sounding signal bandwidth ΔF , that is $\delta t = 1/\Delta F$. This offset also defines the potential range resolution, because, in general, it is equal to the main peak of a signal $s(t)$ after its compression. For waveforms with a large BT-product (compression ratio), the offset components of a signal in Eq. (6) are highly overlapped in time, because the relative time shift is small compared to the pulse duration $\Delta t \ll T_p$, since $T_p = BT \times \Delta t$. That is the offset components of a signal (6) are highly overlapped in time. After their pulse compression, the offset components become orthogonal in time, because their offset peaks have a width equal to the offset size. The obtained orthogonality exists not depending on the spacing between the array elements.

As known, time or frequency offsetting can affect the radiation pattern of a phased array [13, 14]. However, the time offsets introduced in Eq. (6) do not influence the angular-dependent coefficients $A(n, \theta_0)$ (real patterns) for the following reason. A phase shift at a given frequency f , associated with the offset δt , can be written as $\Delta\phi = 2\pi \cdot f \cdot \delta t$. Since the frequency of a sounding signal varies within ΔF , $\Delta\phi = 2\pi$. So, the individual time offset δt (or its multiples) applied to the element wise received signals adds the phase shift 2π (or its multiples) not depending on the direction of arrival of the received signals. Therefore, the introduced time delays in Eq. (6) do not affect the estimated coefficients $A(n, \theta_0)$.

Adding the offsets in the received signal in Eq. (6) allows keeping the same phase relations between its components. So, the time shifts in our calibration technique do not influence the radiation pattern, contrary to the approach in [15], where time delays are also used for phased array calibration. The relative time offset is equal to the width of a compressed signal $s(t)$, that is to the width of the peak of its auto-correlation function ACF_s . It means that after pulse compression, the offset components of a sum signal can be separated in time domain. In turn, this allows the direct measurement of the coefficients $A(n, \theta_0)$ at the output of the pulse compression filter, as shown in Fig. 1.

We assume the pulse compression filter to be matched with the signal $s(t)$. The angular direction is specified as θ_0 , and the output of the matched filter can be written as:

$$\chi_{\theta_0}(\tau) = \int_{-\infty}^{\infty} \left(\sum_{n=1}^N A(n, \theta_0) \cdot s(t + \tau - (n-1) \cdot \delta t) \right) \cdot s^*(t) dt, \quad (7)$$

where the superscript “*” means complex conjugation.

The matched filter output can be written as

$$\chi_{\theta_0}(\tau) = \sum_{n=1}^N A(n, \theta_0) \cdot \int_{-\infty}^{\infty} s(t + \tau - (n-1) \cdot \delta t) \cdot s^*(t) dt. \quad (8)$$

For real signals having a finite length, the integration interval over t is determined by the auto-correlation function of the signal $s(t)$: ACF_S , which is non-zero in $(-T \dots T)$. By expressing the auto-correlation integral in Eq. (8) via the auto-correlation functions of the signal $s(t)$, we obtain:

$$\chi_{\theta_0}(\tau) = \sum_{n=1}^N A(n, \theta_0) \cdot ACF_S(\tau - (n-1) \cdot \delta t). \quad (9)$$

The time integral in Eq. (9) results in the offset auto-correlation functions ACF_S . For a signal $s(t)$ providing good auto-correlation properties (low side-lobes), its normalized discrete ACF can be approximated as a single sample or a single narrow pulse, $ACF_S(\tau) \cong \delta(\tau)$, where the maximal value is equal to 1. Therefore, the ACF can provide the filtering properties in time domain by analogy with the discrete delta function. It is stressed that the approximation on the zero sidelobe level of the ACF is made here for explanation of the calibration method principle that has not been used for modeling or processing of the experimental data presented further in this paper.

We notice that Eq. (9) is not a function of a continuous (can be also discrete) time τ only. It is also a function of discrete time instants $i = n \cdot \delta t$ ($i = \text{round}(\tau/\delta t)$). The number of considered time instants directly corresponds to the number of receiving elements N . Due to the filtering properties of the auto-correlation function, Eq. (9) can be rewritten as:

$$\chi_{\theta_0}(i) = \sum_{n=1}^N A(n, \theta_0) \cdot \delta(i - (n - 1)). \tag{10}$$

The discrete samples (or pulses) in Eq. (10) are not equal to zero only at specific instants which are separated in time. Therefore, the estimations of the coefficients $A(n, \theta_0)$ (the real embedded patterns affected by the coupling effects) can be measured directly at the output of the matched filter at appropriate time instants i , that is

$$\hat{A}(n, \theta_0) = \chi_{\theta_0}(i), \quad \text{for } i = n, \tag{11}$$

where, as we remember, $n = 1 \dots N$ denotes the number of receiving elements, and $i = 1 \dots N$ are the appropriate time samples.

We would like to remind that the real pattern coefficients $A(n, \theta_0)$ are estimated in the operating mode, when all N radar channels are functioning, and the corresponding phase shifters specify each angular direction θ_0 . It means that the presented calibration technique can take into account a large number of effects due to the diffraction, mismatch, variations in elements themselves, etc., which affect

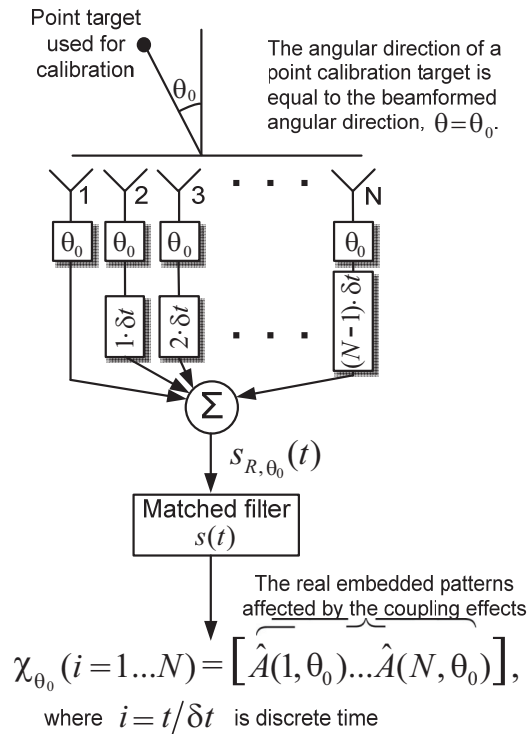


Figure 1. Phased array receiver with the introduced time delays.

the embedded patterns $P_n(\theta_0)$ of the array elements. Therefore, the measured real patterns (coefficients $\hat{A}(n, \theta_0)$) already include the influence of phase shifters and other effects, such as diffraction.

Based on Eqs. (5) and (11), the correcting (calibration) coefficients for each beamformed angular direction θ_0 can be written as

$$C(n, \theta_0) = \frac{P_0(\theta_0)}{\hat{A}(n, \theta_0)}. \quad (12)$$

Since a phased array performs beamforming in a number of angular directions, the result of the calibration procedure in Eq. (12) is shown in the following lookup table having size $[N \times K]$:

$$\mathbf{C} = \begin{bmatrix} C(1, \theta_{0,1}) & C(1, \theta_{0,2}) & \dots & C(1, \theta_{0,K}) \\ C(2, \theta_{0,1}) & C(2, \theta_{0,2}) & \dots & C(2, \theta_{0,K}) \\ \vdots & \vdots & \ddots & \vdots \\ C(N, \theta_{0,1}) & C(N, \theta_{0,2}) & \dots & C(N, \theta_{0,K}) \end{bmatrix}, \quad (13)$$

where each column corresponds to one beamformed angular direction $\theta_{0,k}$, $k = 1, \dots, K$, where K is an overall number of beamformed directions. During the calibration process, the beamformed angular direction and the angular position of a calibration target (point scatterer) are equivalent. The calibration coefficients are inversely proportional to the relative error coefficients $E(n, \theta_0) = 1/C(n, \theta_0)$. Therefore, the relative error matrix \mathbf{E} uniquely defines the calibration matrix \mathbf{C} and vice versa.

In the operating mode, the signals received by different array elements are not shifted in time. After reception, they are corrected by the appropriate calibration coefficients taken from the lookup table in Eq. (13) for a given beamformed angular direction θ_k :

$$s_{R, \theta_{0,k}}^{corr}(t) = \sum_{n=1}^N C(n, \theta_{0,k}) \cdot s_R^n(t), \quad (14)$$

where the superscript ‘*corr*’ stands for ‘corrected’.

3.2. Important Notes

- a) The calibration technique can be applied equally well to arrays of any type of radiating elements. The theoretical pattern of an individual array element is supposed to be known.
- b) The calibration technique can be applied equally well to equidistant and non-equidistant arrays. This is because the relative time offset δt introduced according to the calibration principle makes the received signal components orthogonal in time after their pulse compression not depending on the position vector of the array elements.
- c) The calibration method is suitable for small and medium phased arrays. The bandwidth of a sounding signal is supposed to be reasonably large. In the case of large phase arrays or small bandwidth value, the relative time offsets will result in large time delays along the radar channels, which is impractical from an application point of view. It is noted that transmission lines with the group velocity smaller than the speed of light can be used for implementation of relatively large time offsets to the elementwise received signals. Nevertheless, we do not recommend our technique for large phase arrays.
- d) The calibration method can be easily extended to 2D planar array. It does not require the algorithm modification. The total number of elements should remain N , and the position vector (see Eq. (1)) should describe position of the corresponding 2D array elements. However, the possibility of practical implementation of the delays $\delta t, 2 \cdot \delta t, \dots, (N-1) \cdot \delta t$ significantly limits the use of the proposed method in 2D array applications (N should be reasonably small).
- e) The waveform used for calibration and the waveform used for sounding are not necessarily the same. However, they should occupy the same bandwidth and be radiated at the same carrier frequency. The calibration waveform can have any modulation suitable for pulse compression: linear frequency modulation, phase code manipulation, polyphase coding, etc. It is necessary however to keep in mind that the auto-correlation function (ACF) sidelobes of the waveform used for calibration can,

in some cases, reduce the accuracy of the extracted calibration coefficients and should be estimated in advance.

- f) The introduced time delays can affect the signals during the calibration process. Their influence can be estimated by using the proposed calibration technique when the delays are switched on, and the array is switched off (the sounding signal is sent directly to the receiver channels). The distortion coefficients introduced by the delay lines can be estimated as the amplitude of the signals at the matched filter output for one received pulse.

4. VALIDATION OF THE PROPOSED CALIBRATION TECHNIQUE

The proposed calibration technique has been validated using a fully digital array test-bed in its operating mode. The receiving linear phased array is made of $N = 8$ antennas (patches) spaced by a half-wavelength distance $d = \lambda/2$ from each other. The carrier frequency was equal to 10 GHz. The down-converted signals were digitized and processed. The digit capacity of the analog-to-digital converter was equal to 14 bit. The sampling rate was equal to 125 MHz. The experimental results are presented for a sounding LFM signal. The pulse duration and bandwidth were equal to 320 μs and 40 MHz, respectively. The measurements were carried out by using an active radiator (as a point scatterer) in the far field of the array. The experiment was performed in the anechoic chamber. No window weighting was applied to the received signals. The ideal embedded pattern $P_0(\theta)$ of each array element was described by a cosine function.

The phases of the digitized received signals were initially changed appropriately for each angular direction of the calibration target θ_0 . Then the digitized signals were summed with appropriate offsets $(n - 1) \cdot \delta t$, where n is a number of the receiving channel, $n = 1 \dots 8$. It is equivalent to the proper analog summation described by Eq. (6). The smallest and largest offsets were equal to 25 ns and 175 ns (equivalent to 7.5 m and 52.2 m), respectively. Since the total delay length is rather large, compact transmission lines are advised to be used for practical implementation of our example. The calibration coefficients in Eq. (12) were extracted from the sum signal at the matched filter output (see Fig. 1). After that, the phase and amplitude correction coefficients were applied to the original received signals. One received pulse was used during the calibration technique for each considered angular direction θ_0 within the angular sector $[-40^\circ \dots +40^\circ]$ with a step of 5° .

Figure 2 visualizes the normalized matched filter output (thick black line) for one given angular direction, the components of the output signal (thin colored lines) and the characteristic points (8 black dots) show the estimated coefficients $\hat{A}(n, \theta_0)$ used for calculation of the calibration coefficients by Eq. (12). It is stressed that the characteristic points coincide in time with the zeros of the sidelobes of the interfering components (see the colored lines). Therefore, in our example, the relatively high sidelobes do not affect the estimation of the coefficients $A(n, \theta_0)$.

The calibration procedure provides the calibration coefficients $C(n, \theta_0)$ and the relative error coefficients $E(n, \theta_0)$, which uniquely define each other. The amplitude and phase of the relative error matrix \mathbf{E} is shown in Figs. 3(a)–(b), respectively. The edge effects affect the first and last array elements, where the error amplitudes are higher (Fig. 3(a)). In turn, the phase distortions are higher for the inner elements of the array (Fig. 3(b)). Nevertheless, Fig. 3 proves that the amplitude and phase errors can be evaluated for each given beamformed direction. When evaluated, the errors can be compensated afterwards.

Figure 4 shows the array patterns (functions of the observed angular direction θ) for a number of beamformed directions θ_0 in comparison with the corresponding array factors (black lines). The real array patterns (red lines) before the calibration are reported in Fig. 4(a). The red lines in Fig. 4(b) show the calibrated array patterns after compensation of the phase and amplitude errors. The ideal radiation pattern $P_0(\theta)$ of the individual antenna element (in gray) is represented as the envelope of the array patterns in Fig. 4. A closer inspection of the figures allows the detection of the difference between the non-calibrated and calibrated data.

Figure 5 shows the difference between the real and ideal array patterns as functions of an observed angular direction θ calculated for all the beamformed angular directions $\theta' \in [-40^\circ, \dots, 40^\circ]$ with a step of 5° . The real array patterns are measured. The ideal (theoretical) array patterns are calculated under ideal conditions: in the absence of coupling and parasitic effects, with no difference between

the embedded patterns of the elements, etc. In Fig. 5(a), the average deviation is -37.4 dB for $-90^\circ < \theta < 90^\circ$ (all possible angles) and -38.7 dB for $-50^\circ < \theta < 50^\circ$ (within the -3 dB beamwidth of the individual array element, see Fig. 4). The average deviation in Fig. 5(b), when the phase errors are compensated, is -40.1 dB within $-90^\circ < \theta < 90^\circ$ and -40.7 dB within $-50^\circ < \theta < 50^\circ$. After amplitude compensation, the average deviation values (see Fig. 5(c)) are -41.0 dB and -41.3 dB, respectively. In our example, the amplitude correction is slightly more effective than phase correction. When both amplitude and phase corrections are applied (see Fig. 5(d)), the deviation from the ideal pattern is completely compensated, error levels being below the considered minimal threshold of -50 dB.

We want to stress that the amplitude and phase corrections in our radar test-bed have been implemented by the signal processing means on the received digitized signals. In reality, the

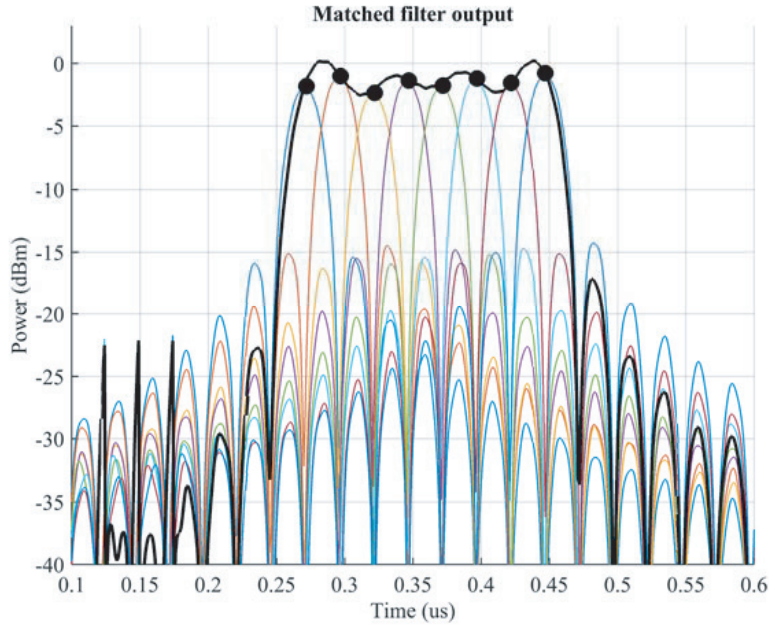


Figure 2. The matched filter output for one given angle (thick black line), its components (thin color lines) and the measured values (8 black dots).

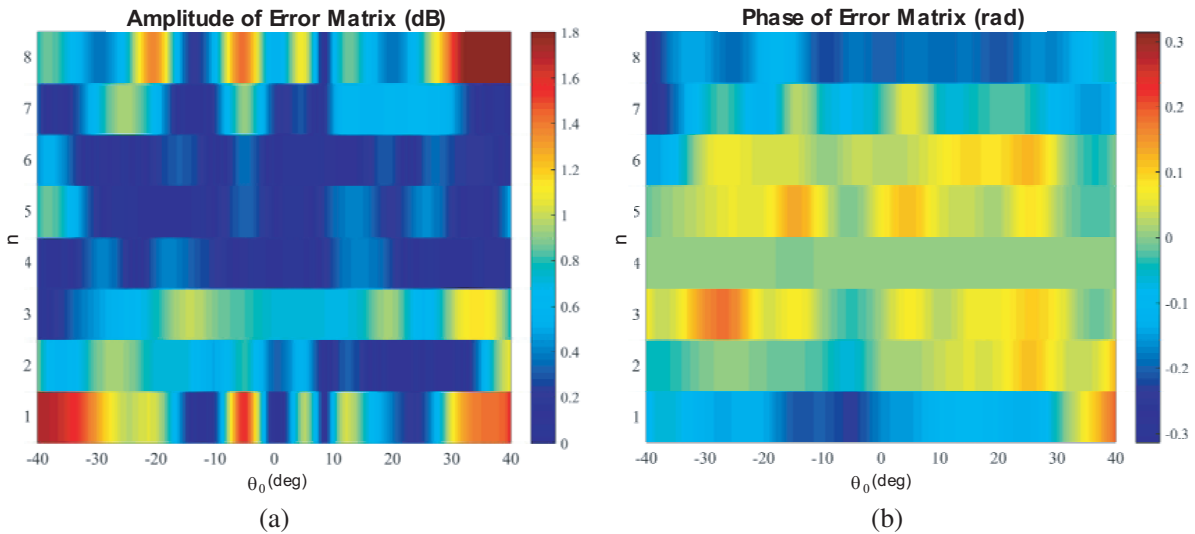


Figure 3. The relative error matrix \mathbf{E} : (a) modulus of the amplitude (dB), (b) phase (rad).

compensation of phase and amplitude errors has to be implemented via phase shifters and attenuators integrated in the system. The proposed calibration technique takes into account static and dynamic errors, because it is executed during the operating mode of the radar. However, the quantization noise of the phase and amplitude control unit cannot be compensated, thereby limits the accuracy of the proposed calibration technique.

5. CONCLUSION

This paper presents a novel simple calibration technique applicable to radars with small- or medium-size phased arrays. Calibration challenges in radar technology are outlined. Solutions based on the proposed technique are proposed and validated by using a radar with an 8-element linear antenna array. The factors limiting the accuracy of the proposed calibration technique are described and analyzed.

The presented calibration technique is implemented directly during the operating mode of a phased array radar, and thanks to that, can efficiently account for a large number of parasitic effects such as mutual coupling between array elements, diffraction phenomena, mismatch, and performance variations at antenna level. As a matter of fact, the developed technique relies on the application of a suitable time offsetting in combination with a switching control between calibration and normal operation of the radar system. Furthermore, the proposed calibration methodology does not require direct measurement of the antenna characteristics or use of matched loading on the array elements. The real embedded patterns of the array elements and mutual coupling effects are taken into account by angular-dependent error coefficients which are derived during the calibration process. The drawback of the proposed calibration technique is that it is not suitable for large arrays, because the implementation of the introduced time offsets is limited from the practical point of view.

Finally, it is stressed that even in case the presented calibration scheme cannot be executed in a controlled laboratory environment, its implementation on the field is still possible by using one dominant point target.

ACKNOWLEDGMENT

This work was carried out in the framework of the project 8.909.2014/K funded by the Ministry of Education and Science of the Russian Federation.

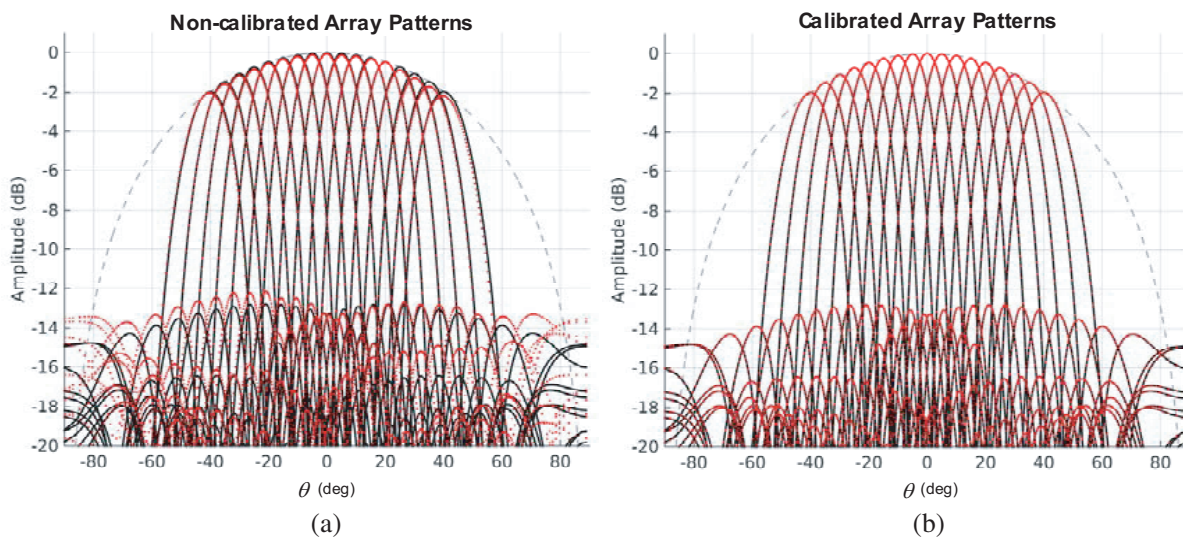


Figure 4. (a) Non-calibrated and (b) calibrated array patterns (in red) in comparison with the array factors (in black); the individual element pattern (in gray), normalized.

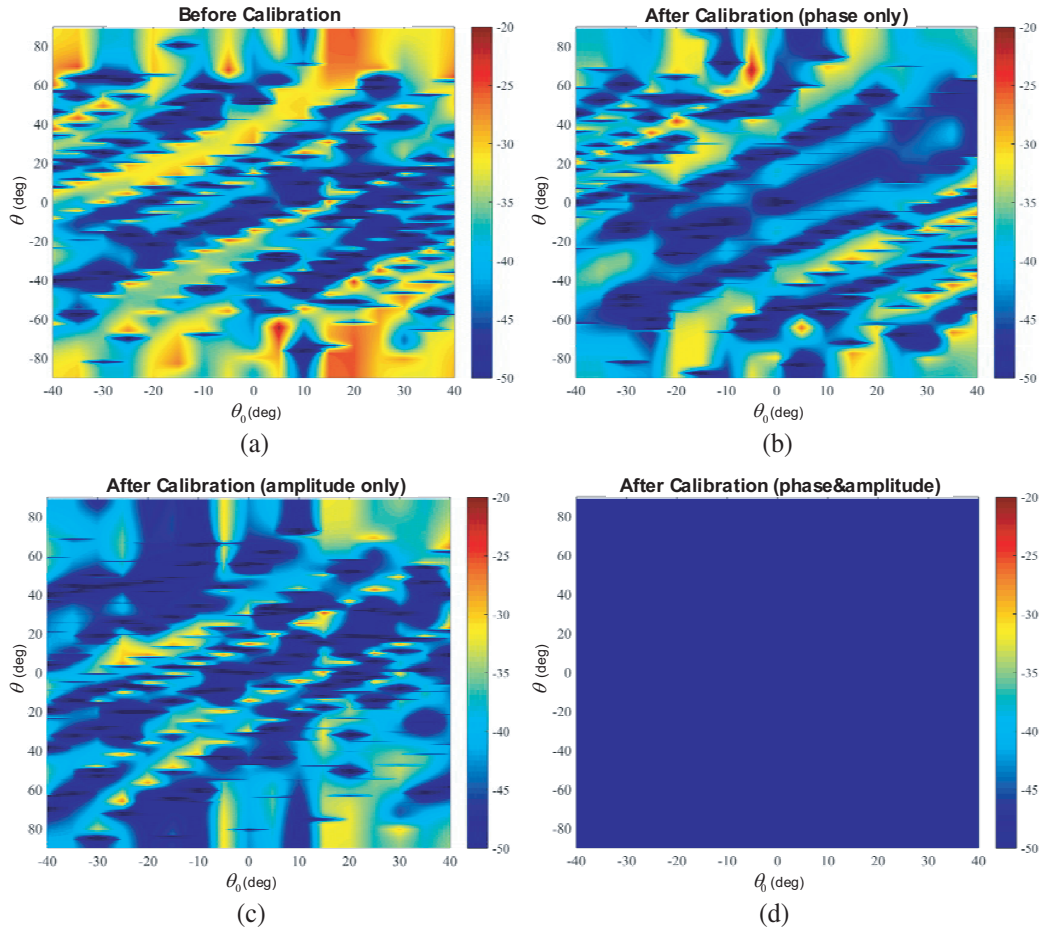


Figure 5. Difference between the real and ideal (theoretical) array patterns (a) before calibration, (b) after phase correction, (c) after amplitude correction and (d) after amplitude and phase correction, (absolute value).

REFERENCES

1. Mailloux, R. J., *Phased Array Antenna Handbook*, 2nd Edition, Artech House, Inc., Norwood, MA, 2005.
2. Hansen, R. C., *Phased Array Antennas*, John Wiley & Sons, Inc., New York, 2009.
3. Caratelli, D. and M. C. Viganó, "Analytical synthesis technique for linear uniform-amplitude sparse arrays," *Radio Science*, Vol. 46, No. 4, RS4001, Aug. 2011.
4. Caratelli, D. and M. C. Viganó, "A novel deterministic synthesis technique for constrained sparse array design problems," *IEEE Transactions on Antennas and Propagation*, Vol. 59, No. 11, 4085–4093, Nov. 2011.
5. Gupta, I. J. and A. K. Ksienski, "Effect of mutual coupling on the performance of adaptive arrays," *IEEE Transactions on Antennas and Propagation*, Vol. 31, 785–791, May 1983.
6. Babur, G., P. Aubry, and F. Le Chevalier, "Antenna coupling effects for space-time radar waveforms: analysis and calibration," *IEEE Transactions on Antennas and Propagation*, Vol. 62, No. 5, 2572–2586, 2014.
7. Tyler, N., B. Allen, and H. Aghvami, "Adaptive antennas: The calibration problem," *IEEE Commun. Mag.*, Vol. 42, No. 12, 114–122, 2004.
8. Sorace, R., "Phased array calibration," *IEEE Transactions on Antennas and Propagation*, Vol. 49,

- No. 4, 517–525, 2001.
9. Tsoulos, G. and M. Beach, “Calibration and linearity issues for and adaptive antenna system,” *IEEE Vehicular Tech. Conf.*, Vol. 3, 1596–1600, May 1997.
 10. Şeker, I., “Calibration methods for phased array radars,” *Proc. of SPIE*, Vol. 8714, 2013, Available at: <http://proceedings.spiedigitallibrary.org/> on 09/08/2013.
 11. Huang, Z. and C. A. Balanis, “Mutual coupling compensation in UCAs: Simulations and experiement,” *IEEE Transactions on Antennas and Propagation*, Vol. 54, 3082–3086, Nov. 2006.
 12. Babur, G., P. Aubry, and F. Le Chevalier, “Space-time radar waveforms: Circulating codes,” *Journal of Electrical and Computer Engineering*, Vol. 2013, Article ID 809691, 8 pages, 2013.
 13. Antonik, P., M. C. Wicks, H. D. Griffiths, et al., “Frequency diverse array radars,” *Proc. IEEE Radar Conf. Dig.*, 215–217, Verona, NY, USA, 2006.
 14. Longbrake, M., “True time-delay beamsteering for radar,” *Proc. of the IEEE National Aerospace and Electronics Conference (NAECON '12)*, 246–249, Dayton, USA, 2012.
 15. Alfred, Q. M., T. Chakravarty, and S. K. Sanyal, “A novel schematic for calibration of large phased array antenna using programmable time-delay units,” *Progress In Electromagnetics Research*, Vol. 65, 81–91, 2006.